Structural and electro-thermal analysis of a magnetic resonant sensor structure based on Lorentz force

A. L. Herrera-May, J. Martínez-Castillo, P. J. García-Ramírez
Research Center for Micro and Nanotechnology, Veracruzana University,
Z.C. 94294, Boca del Río, Ver., México
leherrera@uv.mx, jaimartinez@uv.mx, jagarcia@uv.mx

E. Morales-González
Engineering Faculty of Veracruzana University
Z.C. 94294, Boca del Río, Ver., México
emorales@uv.mx

A. Ramírez-Treviño
CINVESTAV-Guadalajara, Z.C. 45010, Zapopan, Jal., México
art@gdl.cinvestav.mx

W. Calleja-Arriaga
National Institute of Astrophysics, Optics and Electronics
Apdo. 51, Sta. María Tonantzintla, Puebla, México
wcalleja@inaoep.mx
(Recibido: 14 de marzo de 2006; Aceptado: 29 de agosto de 2006)

The structural and electro-thermal analysis of a resonant structure for a magnetic sensor based on MEMS technology is presented in this paper. The effect of squeeze-film damping is included by mean of a theoretical model and using finite element software. In addition, analysis of the dynamic torsional model of magnetic structure is realized. The design of resonant structure considers a hollow rectangular configuration with thin beams of 20μm of width and 1.50μm of thickness suspended over a cavity that takes advantage of the Lorentz force principle allowing the detection of magnetic fields at levels of tens Gauss. The analytical results and simulations with finite element indicate that the vertical displacement has a linear behavior with low power consumption and a maximum Von Mises stress of 20.22MPa with a peak to peak voltage of 2 V.

Keywords: MEMS; magnetic field; Lorentz force; dynamic torsional model; resonant frequency.

1. Introduction

MEMS (Micro-ElectroMechanical Systems) use planar microelectronics fabrication techniques to produce three-dimensional structures, which have both electronic and mechanical functionality. A powerful aspect of MEMS technology is the fact that these structures allow the possibility of combining mechanical actuation with sensing and electronic control, all integrated in a common fabrication technology. MEMS sensors and actuators can be based on a variety of physical, chemical and biological principles [1-2], involving the deflection on the microstructures. Thus, smaller magnetic sensors can be integrated in systems where the space is a constraint.

A variety of applications such as the measurement of the Earth's magnetic field, biosensors for medical diagnosis, as well as rotational speed measurement in navigation, are possible using magnetic field sensors.

Most of the magnetic field sensors exploit the Hall Effect. A major drawback of these sensors related to their low resolution as result of their scattering effects on the surface mobility, as well as the offset and its small dynamic range [3]. According to this, many studies of magnetic sensors have been carried out [4-6]. On the other hand, one important advantage is related to the flexibility in design and fabrication allowing the detection of magnetic fields with a operation range established previously. In this work, the design of a novel configuration of a resonant structure for a magnetic sensor of polysilicon is presented.

2. Description of the sensor

2.1 Principle of operation

The structural configuration for the resonant magnetic sensor is constituted by thin beams with rectangular configuration and two "L" shaped beams. This configuration allows the application of an alternating current (I_L) that will circulate through the beams, and under the influence of a magnetic field a Lorentz force will be

Table 1. Mechanical properties of materials used in the analysis with ANSYS9.0 [7-9].

Mechanical Properties	**Gold**	**Polysilicon**
Young's modulus (GPa)	75	160
Fracture stress (GPa)	0.17	1.21
Poisson's ratio	0.42	0.23
Density (kg/m^3)	19300	2320
Thermal conductivity (W/mK)	315	34
Coefficient of thermal expansion (10^{-6}/°C)	14.20	2.80
Resistivity (Ωm)	$2.88x10^{-8}$	$3.25x10^{-5}$

generated, causing a magnetic torque that provokes it to oscillate (Fig. 1). Ideally, the alternating current operates at the resonant frequency of the structure in order to get the highest magnetic sensitivity.

The Lorentz force, F_R, is given by:

$$F_R = I_L L_z B_x \quad (1)$$

with the length of the largest beam parallel to rotation's axis L_z and the magnetic field parallel to the surface's plane B_x. The structure will oscillate around the rotation axis. For a small rotation, the mechanic torque causes for Lorentz force is given by:

$$T_{field} = 2L_x L_z I_m B_x \sin(2\pi ft) \quad (2)$$

with the length from the end of the structure to the rotation's axis L_x and the peak alternating current I_m.

This torque will produce a deflection of the structure that is limited by the gap of 2.50μm between the structure and the substrate that limits the operating range of the sensor.

2.2 Dimensions and Materials

The dimensions of the structure (in microns) are specified in Fig. 2. The beams were designed with 20μm of width and 1.50μm of thickness, in order to reduce the squeeze-film damping. The material of the structure is polysilicon with gold connection pads. The mechanical properties of the materials used in the simulation are shown in table 1 [7-9]. The structure is adapted so that it oscillates in a torsional vibration mode (first resonant frequency).

Table 2. Resonant frequencies of magnetic sensor obtained by ANSYS9.0.

Vibration mode	**Resonant frequency** (Hz)
1	16016
2	20554
3	41513
4	43577
5	80225

3. FEM analysis

3.1 Modal Analysis

The modal analysis of the structure was realized using a meshing of 1502 Solid95 elements through ANSYS9.0 finite element software. The first five resonant frequencies of the structure (table 2) as well as their first five modal configurations were obtained. The first vibration mode shape is of torsional type and occurred at a frequency of 16016 Hz (Fig. 3).

In Fig. 4 the next four vibration mode shapes are shown, however they do not have suitable mode shapes to use the Lorentz force effect because they don't generate torsional oscillation.

3.2 Electro-thermal analysis

The electro-thermal analysis objective is to obtain the maximum value of the Von Mises stress and the increase of temperature at the structure when a voltage is applied. For this analysis, a meshing of 7921 Solid98 elements with 16462 nodes at the structure was selected. During the simulation with the finite element software an alternating voltage 1 to 4 volt was applied. The Von-Mises stress was obtained in node 4896 (near the beginning of "L" shaped beam). The maximum Von-Mises stress of 80.90MPa for a peak to peak voltage (Vpp) of 4 V was registered (table 3). The maximum stress was below of the polysilicon fracture stress.

The applied voltage causes a temperature increment of 509.1ºC for 3 V and 905ºC for 4 V. These values are near to the gold melting point (1063ºC) as well as to the polysilicon's one (≈1400ºC). This will cause an unstable behavior in the structure. Therefore, is recommended a voltage smaller that 3V. For a Vpp of 2V we obtained a maximum alternating current of 574.0μA that caused low power consumption (≈287μW).

3.3 Air damping analysis

The air damping is a parameter that affects the sensitivity of the magnetic sensor structure [10-11]. If the resonant MEMS operate in a high vacuum behavior the air damping will be diminished considerably [12].

Table 3. Results of the electro-thermal analysis of the structure for magnetic sensor proposed.

Peak to peak voltage (V)	1	2	3	4
Stress in node 4896 (MPa)	5.06	20.22	45.50	80.90
Maximum alternating current (μA)	285.50	574.00	857.00	1141.30
Temperature increment (ºC)	56.60	226.30	509.10	905.00

There is an air gap of 2.50μm that causes a squeeze-film damping when the structure operates in its first vibration mode. Therefore, in order to evaluate this damping an air film with ANSYS9.0 was taken into account with 751 elements Fluid136 and 1502 Solid95 (Fig. 5). In simulation results, the damping ratio was of $46.92\text{x}10^{-2}$ for atmospheric pressure.

3.3.2 Theory

The total squeeze-film damping can be calculated as the sum of the squeeze-film damping of the each beam in motion (parallel and transversal beams), as shown in Fig. 6.

An equivalent gap volume can be used for calculated the squeeze-film damping of each beam, as shown in Fig. 7 for a parallel beam. The pressure drop in the element *dx* is [13]

$$dp = \frac{12\mu_{eff}\,\mathrm{v}_x}{d^2}dx \qquad (3)$$

Here v_x is the equivalent flow velocity in the x-direction in the volume if the velocity is considered constant along the y-axis and μ_{eff} is an approximation of the effective air viscosity [14].

$$\mu_{eff} = \frac{\mu}{1+9.638K_n^{1.159}} \qquad (4)$$

$$K_n = \frac{\lambda}{d} \qquad (5)$$

with the Knudsen number K_n, the viscosity coefficient μ, the air gap d and the mean free path δ that is inversely proportional to static pressure P:

$$\lambda = \frac{P_0}{P}\lambda_0 \qquad (6)$$

with $\lambda_0=64\text{x}10^{-9}$m at atmospheric pressure.

This gives the squeeze-film loss in the element

$$dW_f = vdpdAdt \qquad (7)$$

Integration of Eq. (7) using Eq. (3) gives for two volume element of a parallel beam

$$W_{fp} = 8\int_0^{b/2}\int_0^{Lp}\int_0^{T/4}\frac{12\mu {v_x}^2}{d}dxdzdt \qquad (8)$$

Where, as a result of the vibrating parallel beam and volume continuity,

$$v_x = \frac{x}{d}\delta\omega\cos\omega t \qquad (9)$$

with the vertical displacement of beam δ.

Then the squeeze-film loss of two volume associated with a parallel beam is

$$W_{fp} = \frac{\pi\mu\omega\delta^2 b^3 L_p}{d^3} \qquad (10)$$

with the beam width *b*.

For two volume element of a transversal beam the squeeze-film loss is

$$W_{ft} = 8\int_0^{b/2}\int_0^{Lt/2}\int_0^{T/4}\frac{12\mu {v_z}^2}{d^2}\left(d-\frac{2\delta x}{L_t}\right)dxdzdt \qquad (11)$$

Where, as a result of the vibrating transversal beam and volume continuity

$$v_z = \frac{4\delta xz\omega}{(2d-\delta)L_t}\cos\omega t \qquad (12)$$

Then the squeeze-film loss of the volume associated with a transversal beam is

$$W_{ft} = \frac{\pi\mu\delta^2\omega(4d-3\delta)b^3L_t}{6d^2(2d-\delta)^2} \qquad (13)$$

For small amplitude of vibration $4d-3\delta \cong 4d$ and $(2d-\delta)^2 = 4d^2$, then the Eq. (13) is approximated

$$W_{ft} \cong \frac{\pi\mu\delta^2\omega b^3 L_t}{6d^3} \qquad (14)$$

The total squeeze-film loss W_{fT} considering the parallel and transversal beams in motion is

$$W_{fT} = \frac{\mu\pi\omega\delta^2}{6d^3}\left[b_1^3(6Lp_1+Lt_1+Lt_3)+b_2^3(6Lp_2+Lt_2)\right] \qquad (15)$$

The total energy of the system W_{vT} corresponds here to the sum of the kinetic energy of the parallel beams and the kinetic energy of the transversal beams of the resonant structure. Integrations along the parallel and the transversal beams help us to determine the values of the kinetic energies. The final expression obtained for W_{vT} is

$$W_{vT} = \frac{1}{6}\rho\delta^2\omega^2\left[A_1(6Lp_1+Lt_1+Lt_3)+A_2(6Lp_2+Lt_2)\right] \qquad (16)$$

with the cross-section $A_1=hb_1$ and $A_2=hb_2$, considering the thickness of polysilicon h=1.50μm.

Then the total quality factor related to squeeze-film damping Q_{sqT} is

$$Q_{sqT} = 2\pi\frac{W_{vT}}{W_{fT}} \qquad (17)$$

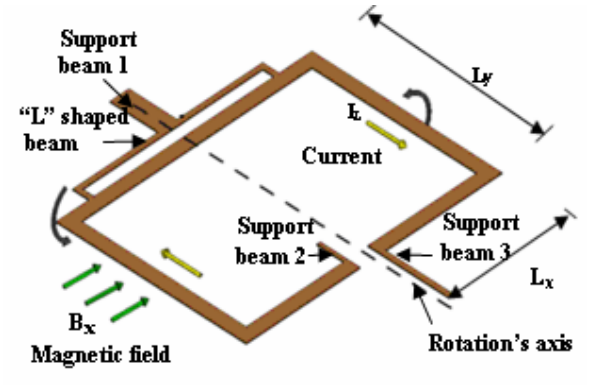

Figure 1. Schematic showing the operation of the magnetic sensor based on MEMS technology.

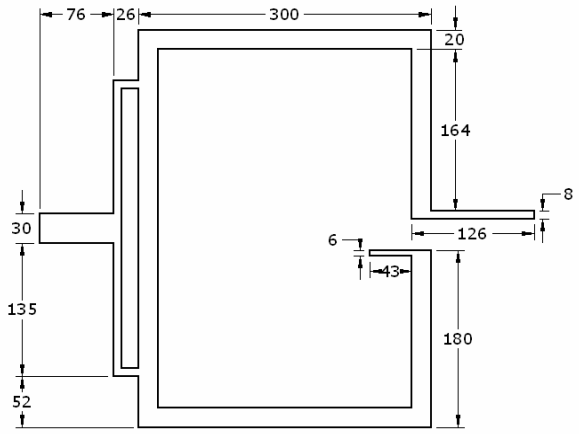

Figure 2. Dimensions (μm) of the resonant magnetic structure.

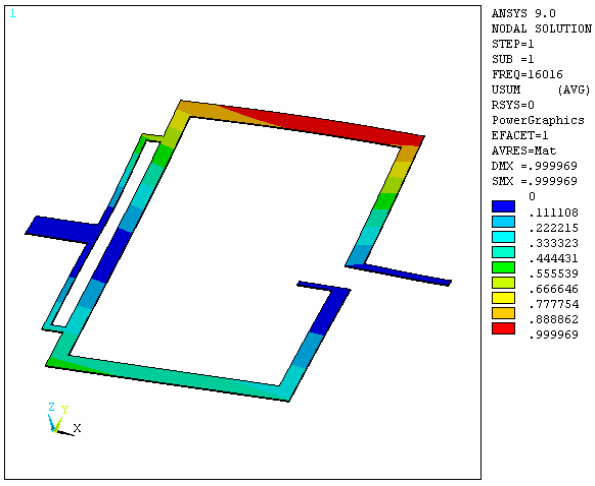

Figure 3. First vibration mode of the magnetic sensor structure.

$$Q_{sqT} = \frac{4\pi f \rho d^3 \left[A_1(6Lp_1 + Lt_1 + Lt_3) + A_2(6Lp_2 + Lt_2)\right]}{\mu\left[b_1^3(6Lp_1 + Lt_1 + Lt_3) + b_2^3(6Lp_2 + Lt_2)\right]} \quad (18)$$

And the ratio damping of the structure can be obtained for

$$\zeta \cong \frac{1}{2Q} \quad (19)$$

Using the equations (18) and (19) and considering the structure of magnetic sensor operating to its first torsional resonant mode obtained with ANSYS9.0 to atmospheric pressure with an air gap of 2.50μm we obtained a damping ratio $\zeta = 30.07 \times 10^{-2}$.

4. Magnetic field analysis

4.1 Analytical

In order to find the torsional resonant frequency for the sensor of analytical form we determined the equivalent torsional stiffness of the sensor and used a single DOF torsional system with a viscous damper. The angular motion equation of the structure under a magnetic field B_x was obtained using the Newton-Euler equation:

$$J_o\ddot{\phi} + C_\phi\dot{\phi} + (k_{\phi T} - M)\phi = 2L_xL_zI_mB_x\sin(2\pi ft) \quad (20)$$

with angular moment-of-inertia of the structure J_o, angular deflection ϕ, angular velocity $\dot{\phi}$, angular acceleration $\ddot{\phi}$, angular damping coefficient C_ϕ, equivalent torsional spring constant of structure $k_{\phi T}$, and the moment M produced by the unbalanced total mass of the structure. The angular damping coefficient can be expressed as $C_\phi = \sqrt{2\zeta J k_{\phi T}}$.

In the underdamped case the undamped torsional resonant frequency f_{tn} and the damped torsional resonant frequency f_{td} are given by:

$$f_{tn} = \frac{1}{2\pi}\sqrt{\frac{k_{\phi T} - M}{J_o}} \quad (21)$$

and

$$f_{td} = \sqrt{1-\zeta^2}\, f_{tn} \quad (22)$$

Due to the configuration of the three support beams the equivalent torsional spring constant of structure, $k_{\phi T}$, is the sum of the torsional spring constant of each support beam,

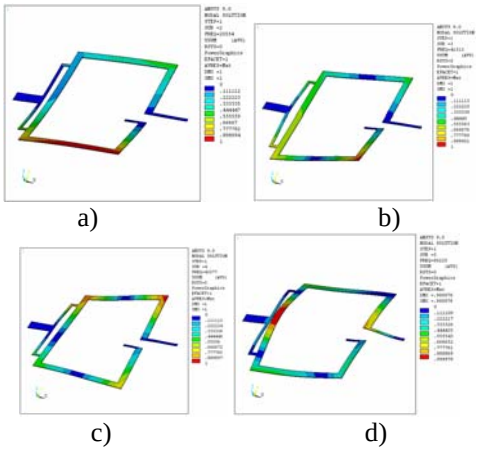

Figure 4. a) Second b) third c) fourth and d) fifth vibration mode shape of the magnetic sensor structure.

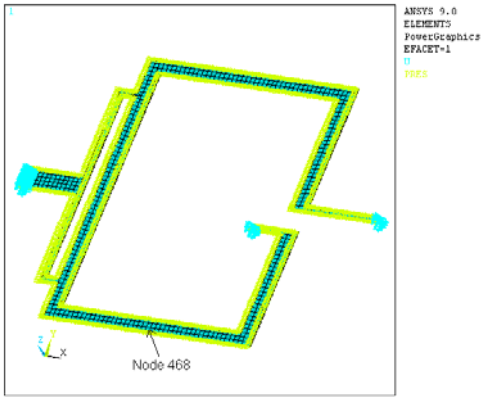

Figure 5. Mesh with 751 elements Fluid136 and 1502 Solid95 for the squeeze-film damping analysis of the magnetic structure.

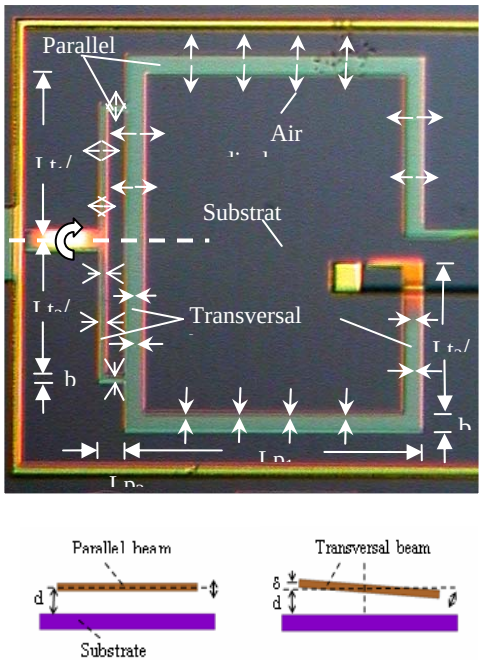

Figure 6. Descriptive view of the torsion mode showing the air displacement, the parallel and the transversal beams, for the resonant structure with one substrate.

$$k_{\phi T} = k_{\phi 1} + k_{\phi 2} + k_{\phi 3} \tag{23}$$

Assuming each torsional beam of length L_{beam} is straight, a uniform cross section and a homogeneous isotropic material that obeys Hooke's law, the torsional stiffness can be expressed as,

$$k_{\phi} = \frac{K_{beam} G}{L_{beam}} \tag{24}$$

with a cross-section dependent factor K_{beam} and shear modulus G is given by:

$$G = \frac{E}{2(1+\nu)} \tag{25}$$

with elastic modulus E and Poisson's ratio ν.

For a beam with a rectangular cross section of wide w_{beam} and thickness t_{beam}, the cross-section shape-dependent factor is expressed as [15]:

$$K_{beam} = \frac{(2a)^3(2b)}{3}\left[1 - \frac{192}{\pi^5}\left(\frac{a}{b}\right) \times \sum_{n=1,3,5,\ldots}^{\infty} \frac{1}{n^5} \tanh\left(\frac{n\pi b}{2a}\right)\right] \tag{26}$$

with $2a = \min(\omega_{beam}, t_{beam})$ and $2b = \max(\omega_{beam}, t_{beam})$.

Considering the dimensions of the three support beams, shown in table 3, the equivalent torsional spring constant is $k_{\phi T} = 3.54\text{x}10^{-8}$ Nm/rad. The angular moment-of-inertia of the structure is $J_o = 21.70\text{x}10^{-19}\,\text{kg}\cdot\text{m}^2$ and the moment is $M = 7.93x10^{-15}$ Nm. Replacing these values in Eq. (21) and Eq. (22), we obtained an undamped torsional resonant frequency f_{tn}= 20,320.83 Hz and a damped torsional resonant frequencies f_{td} of 19,380.36 Hz considering ζ=30.07x10^{-2} (obtained with the theorical analysis of squeeze-film damping).

4.2 Angular deflection and vertical displacement

Under the influence of a magnetic field parallel to the surface plane, the sensor will experience an angular

Table 3. Dimensions and masses of the three supportedbeams of the structure for magnetic sensor.

Number of supported beam	1	2	3
2a (μm)	1.50	1.50	1.50
2b (μm)	30	6	8
Length (μm)	84	63	123
Mass (1x10^{-12}kg)	8.77	1.31	3.42

deflection, which can be found when solving Eq. (20) and considering the initial conditions:

$$\phi(0) = 0 \qquad \text{and} \qquad \dot{\phi}(0) = 0 \tag{27}$$

The solution of Eq. (20) is given by:

$$\phi = C_1 e^{-at}\cos(bt) + C_2 e^{-at}\sin(bt) + C_3\cos(2\pi ft) + C_4\sin(2\pi ft) \tag{28}$$

with

$$a = \frac{C_\phi}{2J_o}\ , \quad b = \frac{1}{2J_o}\sqrt{4J_o k_{\phi T} - C_\phi^2} \tag{29}$$

$$C_1 = \frac{4\pi f L_x L_y I_m B C_\phi}{\left[k_{\phi T} - M - (2\pi f)^2 J_0\right]^2 + (2\pi f)^2 C_\phi^2} \tag{30}$$

$$C_2 = -\frac{1}{b}\left[aC_1 + (2\pi f)C_2\right] \tag{31}$$

$$C_3 = -C_1 \tag{32}$$

and $$C_4 = \frac{2L_x L_y I_m B\left[k_\phi - M - (2\pi f)^2 J_0\right]}{\left[k_\phi - M - (2\pi f)^2 J_0\right]^2 + (2\pi f)^2 C_\phi^2} \tag{33}$$

This angular deflection will cause a vertical displacement at the end of the structure. The amplitude of this vertical displacement z_v can be calculated through the expression

$$z_v = L_x \tan(\phi) \tag{34}$$

4.3 Applications

For the next cases a magnetic field analysis was realized using the response of Eq. (20) and ANSYS9.0 with a Vpp=2V for two damping ratios (ζ=46.92x10^{-2} and ζ=30.07x10^{-2}) and a magnetic field range from 0 to 300 Gauss.

4.3.1 Case 1

In this case we analyzed the amplitude of the vertical displacement in the structure caused by a magnetic field range from 0 to 300G and a Vpp=2V with two damping ratios. We considering the node 468 (Fig. 5) of the structure mesh for ANSYS9.0 and we obtained its vertical displacement (Fig. 8) that shown a linear behavior with respect to the magnetic field applied. Theoretical values of vertical displacement showed a better approximation with ANSYS9.0 for a ζ=46.92x10^{-2}.

4.3.2 Case 2

In this case, magnetic fields B_x of 50, 75, 100 and 150G were applied, with a Vpp=2V for a frequency range from 0 to 30 kHz. A damping ratio of 30.07x10^{-2} was considered and the Fig. 9 shows that as the maximum amplitude is reached near the damped torsional resonant frequency (19380.36 Hz). It is observed that a field of 75 G produces a displacement of 3.99nm and in 150G twice that value.

4.3.3 Case 3

The vertical displacement as a function of frequency of the alternating current and quality factor was graphed in this case. The magnetic field applied was 100G with a maximum alternating current of 574μA. Fig. 10 shows that when the quality factor is increased the resonant frequency approaches the undamped torsional resonance frequency f_{tn} (20320.83 Hz). This is obtained as a result of the reduction of the operating pressure which reduces the squeeze-film damping. For these reason, vacuum packaking is recommended.

6. Conclusions

The structural and electro-thermal analysis of a novel configuration of resonant structure for a magnetic sensor based on MEMS technology with applications in the detection of magnetic fields in levels of tens Gauss operated at atmospheric pressure were realized. The design of resonant structure considers thin beams of polysilicon of 1.50μm thickness and 20 μm of width for diminishing the squeeze-film damping. The structural configuration takes advantage the Lorentz force principle and it oscillates at the first damped torsional resonant frequency. The squeeze-film damping was analyzed and the damping ratio of resonant structure obtained by a theoretical model was of 30.07x10^{-2} and 46.92x10^{-2} using finite element software. The electro-thermal analysis shown that a peak to peak voltage (Vpp) of 2 V caused an increase of temperature (226.3 ºC) smaller that the polysilicon melting point (≈1400ºC). In stress analysis for Vpp=2V was registered a maximum Von Mises stress of 20.22MPa into the "L" shaped beam. This value is smaller that rupture stress of the polysilicon. The analysis of the dynamic torsional model of the structure and the results obtained with ANSYS9.0 showed that the vertical displacement (nm) of structure has a linear behavior with a low consumption power (≈287μW).

Acknowledgments

The authors are very grateful to Jose I. Martínez Lopez from the UNAM, to Ignacio Juarez Ramírez from the INAOE, to Enrique Cabrero Carballo and Edmundo Leyva Jiménez from the Veracruzana University for their help in this work.

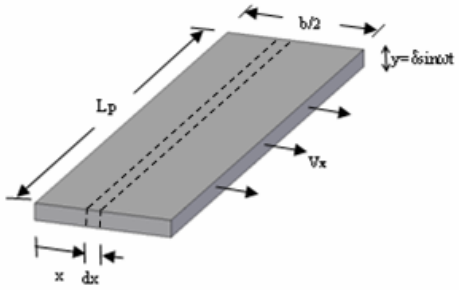

Figure 7. The equivalent squeeze-film volume associated with each parallel beam.

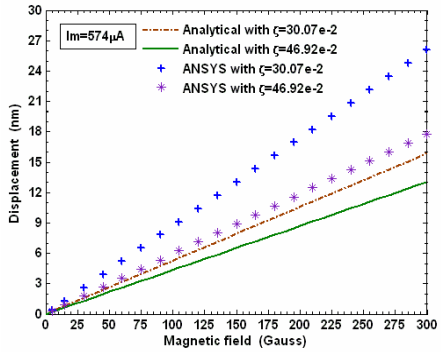

Figure 8. Comparison of vertical displacement (nm) of the magnetic structure obtained by analytical solution and with ANSYS9.0 for fields B_x of 0 to 300 G with a Vpp= 2 V for two damping ratios (ζ=46.92x10^{-2} and ζ=30.07x10^{-2}).

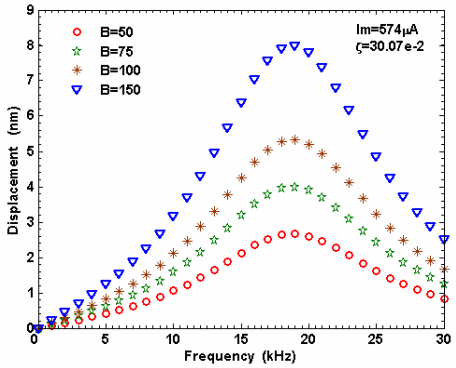

Figure 9. Analytical solution of vertical displacement (nm) of the magnetic structure proposed caused for fields B_x of 50, 75, 100 and 150G with a Vpp=2V in a frequency range of 0 to 30 kHz. In addition was applied a ζ= 30.07x10^{-2}.

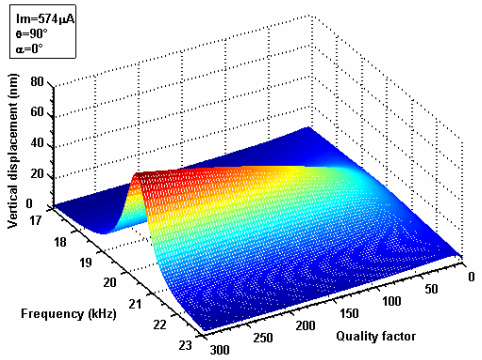

Figure 10. Analytical solution of vertical displacement (nm) for the structure of magnetic sensor versus the frequency and quality factor. The magnetic field applied was 100G with I_m=574μA.

References

[1] [1] M. Elwenspoeck and R. Wiegerink, Mechanical Microsensor, (New York, Springer, 2001).

[2] [2] J. W. Judy, Smart Mater. Struct. **10**, 1115 (2001).

[3] [3] Z. Kadár, A. Bossche, P. M. Sarro, and J. R. Mollinger, Sens. Act. A **70**, 225 (1998).

[4] [4] B. Eyre, K.S.J. Pister, and W. Kaiser, IEEE Electron Dev. Let. **19**, 496 (1998).

[5] [5] R.M. Langdon, J. Phys. E: Sci. Instrum. **18**, 103 (1985).

[6] [6] J. Tucker, D. Wesoleck, and D. Wickenden, NanoTech (2002).

[7] [7] T.R Hsu, Mems & microsystems design and manufacture, (McGraw-Hill, Singapur 2002).

[8] [8] Gad-el-Hak Mohamed, The MEMS Handbook, (CRC Press, Boca Raton, 2001).

[9] [9] MEMSCAP, PolyMUMPs design handbook rev 10.0, URL:http://www.memscap.com/, (2005).

[10] [10] Y.J. Yang and S.D. Senturia, IEEE Solid-State Sens. Actuator Workshop, Hilton Head Island, 76 (1996).

[11] [11] S.S. Mohite, H. Kesari, V.R. Sonti, and R. Pratap, J. Micromech. Microeng. **15,** 2083 (2005).

[12] [12] Z. Kadár, W. Kindt, A. Bossche and J. Mollinger, Sens. Act. A **53,** 299 (1996).

[13] [13] E. Stemme and G. Stemme, Sens. Act. A **32,** 639 (1992).

[14] [14] T. Corman, P. Enoksson and G. Stemme, Sens. Act. A **61,** 249 (1997).

[15] [15] J. W. Judy and R. S. Muller, J. Microelectromech. Syst. **6,** 249 **(**1997).